

# Both live and heat-killed *Bifidobacterium animalis* J-12 alleviated oral ulcer of LVG golden Syrian hamsters by intervening intestinal flora structure

Junhua Jin (✉ [jinjunhua002008@163.com](mailto:jinjunhua002008@163.com))

Beijing University of Agriculture

**Nanqing Jing**

Beijing University of Agriculture

**Fudong Liu**

Inner Mongolia Yili Industrial Group Co., Ltd.; Inner Mongolia Dairy Technology Research Institute Co., Ltd.;

**Ran Wang**

China Agricultural University

**Yan Zhang**

Beijing University of Agriculture

**Jianjun Yang**

China Agricultural University

**Yubing Hou**

Beijing University of Agriculture

**Hongxing Zhang**

Beijing University of Agriculture

**Yuanhong Xie**

Beijing University of Agriculture

**Hui Liu**

Beijing University of Agriculture

**Shaoyang Ge**

China Agricultural University

---

## Article

**Keywords:** *Bifidobacterium animalis* J-12, Oral ulcer, Intestinal flora, Methyl viologen dichloride

**Posted Date:** November 21st, 2022

**DOI:** <https://doi.org/10.21203/rs.3.rs-2292353/v1>

**License:** © ⓘ This work is licensed under a Creative Commons Attribution 4.0 International License.

[Read Full License](#)

---

# Abstract

Live and heat-killed *Bifidobacterium* has been proven to have anti-inflammatory and antioxidant effects. In this study, we evaluated the effects of live and heat-killed *Bifidobacterium animalis* J-12 (J-12) on oral ulceration of LVG golden Syrian hamsters after buccal membrane injection with methyl viologen dichloride. Results showed that interleukin-1 $\beta$ , glutathione and malondialdehyde in serum, downregulated by gavage of live and heat-killed J-12 bacteria. The J-12 live and heat-killed bacteria can reduce the expression of matrix metalloproteinase-9 by reducing the expression of nuclear factor kappa-B, thus reducing the expression of anti-inflammatory factors lipoxinA4 and prostaglandinE2. Reducing the expression of caspase-3 and adenosine diphosphate ribose polymerase resulted in a reduction of ulcer tissue DNA damage. In addition, regulating the structure of intestinal flora prevented the process of oral ulcer formation. This study shows that J-12 can reduce the risk of oral ulcer formation while also having a positive effect on inhibiting existing oral ulcer growth.

## Introduction

An oral ulcer is a common oral mucosal disease with high incidence and wide coverage. The aetiology of this disease is complex with potential inducing factors including mechanical damage, immune dysregulation, genetic predisposition, hormonal influence, nutritional imbalance, infection, allergy, and stress. These factors directly or indirectly destroy the balance between oxidative and antioxidant systems in the human body<sup>1</sup>. Studies have shown that oral health is closely related to oral microbiota<sup>2</sup>, and restoring the balance of oral microbiota in the ulcer site may be a new treatment for an oral ulcer<sup>3</sup>.

Probiotics are live microorganisms that provide health benefits when ingested by improving or restoring the gut flora<sup>4</sup>. The combination of *Bacillus subtilis*, *Bifidobacterium bifidum*, *Lactobacillus acidophilus*, and *Enterococcus faecalis* can alleviate experimental oral mucositis in immunosuppressed rats<sup>5</sup>. The consortium of *Bifidobacterium longum*, *Lactobacillus lactis*, and *E. faecalis* has been shown to significantly enhance the immune response of patients and reduce the severity of oral mucositis caused by radiotherapy and chemotherapy in nasopharyngeal carcinoma by changing the intestinal flora<sup>6</sup>. After two weeks of application, the mixed preparations of *B. longum*, *Lactobacillus bulgaricus*, and *Streptococcus thermophilus* significantly reduced the pain level of *Candidia*-associated stomatitis and hyperaemia of lingual mucosa<sup>7</sup>. In addition, Mimura et al. has found that the synergistic treatment of oligofructose, lactic acid bacteria, and *Bifidobacterium* can reduce the pain incurred by an oral ulcer<sup>8</sup>.

Some strains of *Bifidobacterium animalis* have been shown to have anti-inflammatory and antioxidant effects, where the early intervention of *B. animalis* 420 helps to improve liver immune homeostasis and liver injury in mice with experimental autoimmune hepatitis<sup>9</sup>. In addition, *L. acidophilus* and *B. animalis* can play an effective anti-inflammatory role by regulating the toll-like receptor 2-mediated nuclear factor kappa-B(NF- $\kappa$ B) and mitogen-activated protein kinase signalling pathways in inflammatory intestinal epithelial cells<sup>10</sup>. In the mouse colitis model induced by dextran sulphate sodium, *B. animalis* XLTG11

significantly decreased the levels of proinflammatory cytokines and increased the levels of anti-inflammatory cytokines<sup>11</sup>. In addition, the exopolysaccharide fractions of *B. animalis* RH isolated from the faeces of a centenarian from Guangxi Province yielded direct and effective antioxidant activities<sup>12</sup>.

A large amount of published data indicates that agents containing dead cells and their metabolites exert relevant biological responses. In many cases, these are similar to those observed with live cells<sup>13</sup>. This is due to lipoteichoic acid, peptidoglycan, and extracellular polysaccharide, which are released during the heat inactivation of live cells. These are the key materials to immunomodulatory and antagonistic pathogenicity<sup>14</sup>.

Thus, using probiotics to manage oral ulcers is becoming a preferred treatment. Currently, there are few studies on the intervention effects of *B. animalis* on oral ulcers. In this study, an oral ulcer model was established in LVG golden Syrian hamsters (golden hamsters) by buccal injection of methyl viologen dichloride<sup>15</sup>. We explored the use of J-12 to regulate intestinal homeostasis and its ability in improving oral ulcers by gavage. We also examined the potential anti-inflammatory and antioxidant effects of the live and heat-killed strains of *B. animalis* and compared their efficacy against one another. Conclusively, we looked at the possible activity that *B. animalis* had in the intervention of oral ulcer formation.

## Results

### HE staining of mucosal tissue section

As shown in Fig. 1, in the Normal group, the structure of the epidermis was complete, the content of collagen fibres in the dermis was rich, and a large number of muscle fibres in the subcutaneous muscle layer were visible without obvious inflammation. Compared to the Normal group, the epidermis and dermis cells in the Model group were necrotic, and the nuclei were fragmented or dissolved. There was severe oedema in the subcutaneous tissue and loose arrangement of connective tissue accompanied by scattered inflammatory cell infiltration and more bleeding. This indicated the successful modelling of an oral ulcer. In the J-12L group, there were more newly formed muscle fibres in the subcutaneous tissue accompanied by a small amount of proliferative connective tissue and scattered inflammatory cell infiltration. Moderate oedema and a loose arrangement of connective tissue were also observed, but a local epidermal layer was absent. The results of the J-12D group were similar to those of the J-12L group, although there was no local loss of epidermis, only a small amount of capillary congestion and dilation.

### Levels Of Oxidation Factor In Serum

Superoxide dismutase (SOD ) was discovered half a century ago. Subsequently, SOD was well identified as the first line of defence against oxygen free radicals<sup>16</sup>. Reactive oxygen species, namely superoxide and hydrogen peroxide formed by a certain level of physiological oxidative stress in aerobic organisms, can cause lipid peroxidation and cell damage. Among them, hydrogen peroxide can be reduced by

glutathione GSH with antioxidant function<sup>17</sup>. In addition, lipid peroxidation is enhanced in the process of oxidative stress, leading to the generation of lipid peroxidation products such as malondialdehyde MDA, which can be attached to autologous biomolecules, thereby generating new self-epitopes and inducing potential adverse biological reactions<sup>18</sup>. Therefore, the increase in SOD and GSH suggests that the body stimulates the increase of antioxidants due to oxidative stress. MDA reflects the damage degree of oxidative stress. As shown in Fig. 2, compared with the Normal group, the GSH level in the serum of the Model group was significantly increased ( $P < 0.05$ ), and the levels of GSH in the J-12L and J-12D groups were significantly lower than those in the Model group. The MDA level in the Model group was significantly higher than that in the Normal group, and the MDA levels in the J-12L and J-12D groups were significantly lower than that in the Model group ( $P < 0.05$ ). There was no significant difference in SOD levels among the four treatment groups. The results showed that both J-12 dead bacteria and J-12 live bacteria could reduce the damage degree of oxidative stress in golden hamsters and thus reduce the level of antioxidant substances in the body.

## Levels Of Antioxidant Factors In Mucosal Tissues

LipoxinA4 (LXA4) is a double-acting mediator that activates specific cellular pathways through FPR2/ALX, thereby producing anti-inflammatory and pro-resolution effects<sup>19</sup>. Compared with the Normal group, the LXA4 level in the Model group was increased to a certain extent, and the LXA4 level in the J-12L and J-12D groups was significantly decreased compared with the Model group ( $P < 0.05$ ). prostaglandin E2 (PGE2) not only reduces inflammation but also has significant therapeutic potential for tissue regeneration through macrophages<sup>20</sup>. As can be seen in Fig. 3, compared with the Normal group, PGE2 levels in the Model group and the J-12D group were significantly increased ( $P < 0.05$ ). The level of PGE2 in the J-12 L group had no significant change but was slightly higher than that in the Normal group.

## Levels Of Proinflammatory Cytokines In Serum

Interleukin-1 $\beta$  (IL-1 $\beta$ ) is a major stimulator of regional and systemic inflammation and a major proinflammatory mediator<sup>21</sup>. Interleukin-6 (IL-6) is a typical cytokine to maintain homeostasis. When homeostasis is disrupted by infection or tissue injury, IL-6 is produced immediately and helps the host defend against this emergent stress by activating the acute phase and immune response<sup>22</sup>. As can be seen from Fig. 4, the level of IL-1 $\beta$  in the Model group was significantly higher than that in the Normal, J-12L, and J-12D groups. The results indicated that the J-12 treatment had a certain reduction effect on the level of inflammation. The level of IL-6 in the Model group was significantly higher than that in the Normal group ( $P < 0.05$ ), IL-6 levels in the J-12L and J-12D groups were significantly higher than those in the Normal group ( $P < 0.05$ ), and the level of IL-6 in the Model group was higher than that in the Normal group.

## Immunohistochemical Results Of Mucosal Tissues

The matrix metalloproteinase-9 (MMP-9) gene promoter has a binding site for NF- $\kappa$ B<sup>23</sup>. NF- $\kappa$ B is an important transcription factor, and activation of its signalling pathway can initiate an inflammatory response<sup>24</sup>. Previous studies have shown that MMP in Caco-2 monolayer can participate in the increase of intestinal permeability induced by MMP-9 through the activation of NF- $\kappa$ B<sup>25</sup>. In the response of aluminium-induced increase of TJ permeability in HT-29 intestinal epithelium, NF- $\kappa$ B-mediated upregulation of MMP-9 exists<sup>26</sup>. 15-Deoxy-D12 and 14-prostaglandin J2 inhibit MMP-9 expression induced by 12-O-tetradecanoylphorbol-13-acetate by regulating NF- $\kappa$ B/AP-1 activation in MCF-7 cells<sup>27</sup>. In conclusion, the expression of MMP-9 mediated by NF- $\kappa$ B upregulation is positively correlated with the disease. In this study, the expression of NF- $\kappa$ B and MMP-9 in the ulcer mucosa of the golden hamster oral ulcer model was detected. It can be seen from Table 1 that there are significant differences between the Normal group and the Model, J-12L, and J-12D groups ( $P < 0.05$ ). The levels of NF- $\kappa$ B and MMP-9 in the J-12 treatment group were lower than those in the Model group, indicating that the J-12 intervention has a positive effect on the reduction of inflammation levels.

Table 1  
Immunohistochemical scoring table

	<b>NF-<math>\kappa</math>B</b>	<b>MMP-9</b>	<b>Caspase-3</b>	<b>PARP</b>
Normal	0(-)a	0(-)a	0(-)a	0(-)a
Model	3.7(++b)	2.35(+b)	2.74(+b)	5.2(+++)b
J-12L	2.48(+b)	2(+b)	1.29(+c)	3.95(++b)
J-12D	2.36(+b)	1.95(+b)	0.74(+c)	1.92(+c)

Data are presented as means, one-way ANOVA was used to analyze statistical differences. Different letters indicating significant differences ( $P < 0.05$ ).

Apoptosis is a stage of oral wound healing<sup>28</sup>, although excessive apoptotic cells will increase the release of high mobility group box-1 (HMGB-1)<sup>29</sup>. HMGB-1 is considered an important promoter of diseases such as coronary artery disease<sup>30</sup>, local<sup>31</sup> and systemic inflammation<sup>32</sup>, and cancer<sup>33</sup>. Caspase-3 is recognised as an important effector protease, which is cleaved and activated during apoptosis<sup>34</sup>. Caspase-3 in turn cleaves a variety of cellular substrates, most notably adenosine diphosphate ribose polymerase (PARP). PARP can repair single-stranded DNA damage, and cleaved PARP is an important marker of cell apoptosis<sup>35</sup>. As can be seen from the quantitative scores in Table 2, the Model, J-12L, and J-12D groups were significantly different from the Normal group ( $P < 0.05$ ). The expression levels of caspase-3 and PARP in the Model group were the highest among the four groups, which were significantly different from those in the J-12 group ( $P < 0.05$ ), indicating that the Model group suffered the most severe DNA damage, and that J-12 intervention could alleviate DNA damage caused by modelling.

# The Diversity And Composition Of The Bacterial Community

The dominant bacterial community in the oral cavity of golden hamsters is consistent with the research results of Jin.et al.<sup>36</sup>, which includes *Firmicutes*, *Bacteroidota*, *Proteobacteria*, and *Fusobacteriota* that can be seen in Fig. 6a.

Among these, Fig. 6c shows that *Bacteroidetes* and *Firmicutes* were the dominant intestinal flora. This result is consistent with the results of previous studies<sup>37</sup>.

It can be seen from Fig. 6a and c that there is no difference in the dominant flora of oral and intestinal microbiota in the phylum level among the four groups of samples, with differing relative abundance. To determine whether the four treatments caused significant differences in the structure of the oral and intestinal microbiota of golden hamsters, non-metric multidimensional scaling (NMDS) was performed. This was based on a weighted-normalized-unifrac algorithm at the species level, with results shown in Fig. 6b and d. There was a large overlap between samples from different treatment groups of golden hamster oral microbiota, indicating that the four groups of samples had similar species without significant differences. However, there were significant differences in the structure of intestinal flora between the Model group and the Normal group at the species level.

To determine the source of the above differences, a bacterial species visual circle map was constructed(Fig. 7A and B). Bacterial species with a large difference in relative abundance amongst groups were statistically analysed. Figure 7C and D listed the bacterial species with significant differences in relative abundance among oral and intestinal dominant bacterial species.

Additionally, it can be seen from Fig. 7C and D that the J-12D group and the J-12L group have the ability to regulate the changes in oral and intestinal flora abundance caused by oral ulcers, with the regulatory ability of the J-12D group being stronger than that of the J-12L group.

To further study both the relationship between the changes in oral and intestinal bacterial communities and the indicators caused by the four treatments, a distance-based redundancy analysis (db-RDA) was conducted using the Bray-Curtis algorithm. As shown in Fig. 7E and F, GSH, MDA, NF-κB, and MMP-9 had a pronounced influence on the community structure of oral microbiota in the order of GSH > MDA > NF-κB > MMP-9. GSH, MDA, and PGE2 had a notable influence on the structure of the intestinal microbiota community in the order of GSH > MDA > PGE2.

The top 50 species were selected. The Spearman correlation coefficient was used to evaluate similarities and both inflammatory and immune factors. As can be seen from Fig. 8a and b, MDA has a strong correlation with oral and intestinal flora. In the oral microbiota heat map, *Streptococcus respiraculi* had the strongest correlation with inflammatory and immune factors and was positively correlated with LXA4, MDA, GSH, and NF-κB. *Bifidobacterium pseudolongum* was positively correlated with caspase-3, MMP-9, PARP, and NF-κB. *Uncultured- bacterium - G - Leibacterium*, *Lactobacillus - reuteri*, *Unclassified - g -*

*Lactobacillus*, *Unclassified -g - bifidobacterium*, *Unclassified - F - Eggerthellaceae*, *Uncultured - bacterium - g - enterorhabdus* were negatively correlated with MDA and GSH.

## Discussion

### Effects of *Bifidobacterium animalis* J-12 on oral lesions

Probiotics, especially those from *Lactobacillus*, can stimulate the migration and proliferation of fibroblasts during wound healing<sup>38</sup>. The formation of fibrous connective tissue is a marker of wound repair<sup>39</sup>. According to the results of HE staining of the oral mucosa of golden hamsters (Fig. 1), there was no abnormality in the Normal group. Epithelial cell necrosis and nuclear fragmentation were observed in the Model group, and new muscle fibres and connective tissue proliferation were observed in the J-12L and J-12D groups. It can be inferred that J-12 is beneficial to the healing of oral ulcer in golden hamsters.

There is no uncertainty that J-12 is a probiotic. Studies have shown that probiotics interact with and attach to the gastrointestinal mucosa and gut-associated lymphoid tissues, which are important components of immune cells<sup>40</sup>. During inflammation, as probiotics interact with the gastrointestinal mucosa, the symbiotic microbiota express antimicrobial peptides and activate the toll-like receptor pathway. They induce the production of chemoattractant factors and also regulate the function of dendritic cells and T lymphocytes to promote wound healing<sup>41</sup>.

In addition to this mechanism, probiotics and commensals in the digestive system exhibit a microbe-gut-brain axis mechanism in which neurotransmitters, in the form of oxytocin, are mediated through the vagus nerve to the central nervous system or through blood vessels to affect the human immune system. The use of probiotics may improve the wound-healing process by increasing the regulation of oxytocin in the microbial-gut-brain axis that is conducted via the vagus nerve. Improved systemic oxytocin regulation can upregulate keratinocyte and fibroblast activity to form extracellular motifs<sup>42</sup>.

### Effects Of J-12 On Oxidative Stress

In this experiment, the oxygen free radical damage method was used to model oral ulcers of golden hamsters. MDA in serum can directly express the severity of oxidative damage of golden hamsters, while SOD and GSH can reflect the intensity of the body's stress response in reaction to oxidative damage. We observed significant differences in GSH and MDA levels among all groups ( $P < 0.05$ ). The levels of GSH and MDA in the Model group were significantly higher than those in the Normal group, and the levels of MDA and GSH in the J-12L and J-12D groups were lower than those in the Model group. In addition, the levels of MDA in the J-12L and J-12D groups were significantly different from those in the Model group ( $P < 0.05$ ). These results indicate that the intervention of J-12 bacteria can reduce the oxidative damage of golden hamsters, by J-12 having a positive effect on reducing the oxidative damage of the body.



Caspase-3 and PARP are proteins related to apoptosis. In this study, the expression of these two proteins in the oral ulcer tissue of golden hamsters was detected by immunohistochemistry and scored. As can be seen from the quantitative scores in Table 2, the Model, J-12L, and J-12D groups were significantly different from the Normal group ( $P < 0.05$ ). The model of the oral ulcer was successfully established by injection of methyl viologen dichloride into the buccal membrane. The expression levels of caspase-3 and PARP in the Model group were the highest among the four groups, indicating that the Model group suffered the most severe DNA damage. The J-12 intervention reduced the protein expression of caspase-3 and PARP compared to the Model group, indicating that the J-12 intervention could alleviate DNA damage caused by modelling.

## Effects Of J-12 On Immune Response

As can be seen from Fig. 3A, compared with the Normal group, the level of LXA4 in the Model group increased without significant difference. In addition, the levels of LXA4 in the J-12L and J-12D groups were significantly lower than those in the Model group ( $P < 0.05$ ). These results indicated that both dead and live J-12 bacteria could reduce the level of inflammation in vivo, resulting in the reduction of LXA4 activation.

As can be seen in Fig. 3B, compared with the Normal group, PGE2 levels in the Model and J-12D groups were significantly increased ( $P < 0.05$ ). The level of PGE2 in the J-12 L group had no significant change but was slightly higher than that in the Normal group. The Model group had the highest level of PGE2, indicating that they were the most seriously injured by inflammation. Due to the intervention of J-12, the inflammation level was reduced in golden hamsters, so the expression of PGE2 in the J-12 treatment group was lower than that in the Model group.

In this study, there was no significant difference in the level of IL-6 between the Normal group and the Model group, which indicated that the inflammatory response caused by methyl viologen dichloride spermatogenesis did not completely initiate the IL-6-related pathway. Su et al.<sup>43</sup> proved that there was a negative correlation between IL-6 and Candidatus Saccharimonas in a diabetic nephropathy rat model. In this study, there was no significant difference between the Model and Normal groups and the relative abundance in the Model group was significantly higher than that in the J-12 treatment group ( $P < 0.05$ ). Therefore, the possibility that Candidatus Saccharimonas inhibited IL-6 production could not be excluded.

The expression of IL-1 $\beta$  in the serum of each group was in line with the expected experimental results. Notably, the intervention of J-12 dead bacteria and live bacteria could reduce the expression of proinflammatory factors in golden hamsters. Both NF- $\kappa$ B and MMP-9 are associated with inflammation. According to Table 1, there are significant differences between the Normal group and the Model, J-12L, and J-12D groups ( $P < 0.05$ ). This indicates that the model was successfully established by buccal membrane injection of methyl viologen dichloride, which initiated the inflammatory reaction in golden hamsters. In this study, the J-12 intervention reduced the level of NF- $\kappa$ B and MMP-9 in golden hamsters compared to the Model group. It can be concluded that the J-12 intervention has a positive effect on the

reduction of the inflammatory response of golden hamster oral ulcers that have been caused by buccal injection of methyl viologen dichloride damaging free radicals. This result is consistent with the relationship between NF-κB and MMP-9 reported in previous studies<sup>23</sup>.

## Effects Of J-12 On Oral And Intestinal Microorganisms

The mouth is considered to be one of the largest microbial pools in the human body<sup>44</sup>. Dysregulation, colonisation, and translocation of oral microbiota are essential for carcinogenic function. Multiple potential mechanisms of oral microbial carcinogenesis have been reported, including excessive inflammatory response, host immune suppression, promotion of malignant transformation, anti-apoptotic activity, and secretion of carcinogens<sup>45</sup>. In this experiment, *S. respiraculi* and *Fusobacterium nucleatum* subsp. *polymorphum* are two types of bacteria that increased significantly in the mouth of golden hamsters in the Model group.

*Fusobacterium nucleatum* (*F. nucleatum*) participates in the formation of typical dental plaque and causes periodontal disease<sup>46</sup>. It is considered to be a key promoter of colorectal cancer<sup>47</sup>. *S. respiraculi* is considered a new genus of *Streptococcus*<sup>48</sup>, which is lacking studies related to disease. As can be seen from Fig. 8a, this bacterium is positively correlated with LXA4, MDA, GSH, and NF-κB, so it may cause disease by triggering inflammation and oxidative damage. It can be proven that the dysregulation of oral flora caused by oral ulcers is a threat to oral health. However, the relative abundance of oral microbiota in the golden hamsters treated with J-12 was close to the normal level, indicating that J-12 can regulate the dysregulation of oral microbiota while reducing the incidence of oral and systemic diseases.

*Bacteroides dorei* is a kind of intestinal microorganism isolated from human faecal samples<sup>49</sup>, which can inhibit the growth of *Clostridium difficile* and reduce the production of LPS and atherosclerosis<sup>50</sup>. In animal experiments, mice inoculated with *B. dorei* are protected from influenza infection<sup>51</sup>. It is also negatively correlated with SARS-CoV-2<sup>52</sup>. In this study, *B. dorei* was detected in the mouth, which is presumed to be responsible for the mobility of microorganisms in the environment. Further experiments are needed to determine whether *B. dorei*, a beneficial intestinal bacterium, can maintain its physiological activity after colonising the mouth.

The gut contains some of the most immune cells in the body compared to any other organ. Intestinal bacteria and their metabolites can regulate the immune system through the promotion and maturation of immune cells and by maintaining the normal development of immune functions<sup>53</sup>. In this study, the intestinal bacteria significantly regulated by gavage were *Allobaculum*, *Candidatus Saccharimonas*, and *Clostridia UCG-014*. The effects of J-12L and J-12D on the abundance of these three kinds of bacteria were consistent. *Allobaculum* and *Clostridia UCG-014* levels were significantly different between the Model group and the Normal group ( $P < 0.05$ ). Compared to the Model group, the J-12 intervention significantly increased the relative abundance of *Allobaculum* while decreasing the relative abundance of *Candidatus Saccharimonas* and *Clostridia UCG-014*, which were close to the Normal group.

*Allobaculum* has been identified as a producer of short-chain fatty acids (SCFAs) and has a negative correlation with different proinflammatory markers<sup>54</sup>. High-fat feeding decreased the abundance of *Allobaculum* in mice<sup>55</sup>, with *Allobaculum* negatively correlated with fasting blood glucose<sup>56</sup>. *Prevotella histicola* MCI001 treatment may have prevented arthritis by increasing the relative abundance of the *Allobaculum* genus<sup>57</sup>.

*Candidatus Saccharimonas* is an opportunistic pathogen that is significantly elevated in the gut of patients with gout<sup>58</sup>. Similarly, Su et al. showed that *Candidatus Saccharimonas* was significantly increased in a diabetic nephropathy rat model<sup>43</sup>. Bruna et al.<sup>59</sup> showed that *Candidatus Saccharimonas* was the dominant bacterium associated with inflammatory mucosal diseases, which may be the key cause of glia-associated carcinogenesis, although further studies are needed.

*Clostridia UCG-014* is a proinflammatory bacterium<sup>60</sup>. The data from Dong et al. showed that *Clostridia UCG-014* may play a significant, positive role in type 2 diabetes mellitus, and have a strong positive correlation with fasting blood glucose levels<sup>56</sup>.

Currently, except for *F. nucleatum* and *B. dorei*, the bacteria with significant changes in this study lack direct experiments to prove their effects. Through association analysis, MDA and microbiota had the strongest correlation, which was consistent with db-RDA results. However, this result was not explained by relevant reports in the existing research literature. *Bifidobacterium pseudolongum* was positively correlated with caspase-3, MMP-9, PARP, and NF- $\kappa$ B in the heat map analysis of this experiment (Fig. 8b), indicating that *B. pseudolongum* has the potential to promote inflammation and aggravate DNA damage. At the same time, this result also indicated that the *Bifidobacterium* species had specificity, and the effect of strains could not be generalised.

## Conclusions

The results of this study show that it is feasible to intervene in oral ulcer growth by gavage of live and heat-killed *Bifidobacterium animalis* J-12. The intervention mechanism of this experiment involved J-12 live bacteria and J-12 heat-killed bacteria intervening in oral ulcer growth by regulating intestinal flora, with J-12 heat-killed bacteria showing the best effect. Both J-12 live bacteria and J-12 heat-killed bacteria can reduce the level of oxidative stress injury, with no significant difference between the two. This indicates that J-12 live bacteria and J-12 heat-killed bacteria both have indirect anti-inflammatory and antioxidant effects. In this study, J-12 promoted the healing of oral ulcers caused by methyl viologen dichloride through three pathways. The first is the oxidative stress pathway. By reducing the expression of NF- $\kappa$ B, the expression of MMP-9 was downregulated, which reduced the level of inflammation. Second, the expression of caspase-3, apoptosis-related protein, and DNA repair protein PARP was decreased, and the cell damage caused by methyl viologen dichloride was alleviated. Finally, by reducing the relative abundance of intestinal pathogenic bacteria and upregulating the relative abundance of beneficial bacteria, the homeostasis of intestinal flora could be maintained, the gastrointestinal barrier could be enhanced, and the immune system could be regulated.

## Methods

### Bacterial strain and culture condition

*B. animalis* subsp. *Lactis* J-12 strain (J-12, CGMCC NO.25005) is a strain that was originally isolated from the faecal matter of a 1-month-old infant (vaginal delivery and breastfed). J-12 was incubated anaerobically in modified MRS medium at 2% (v/v) for 12 h at 37°C (three generations). The bacterial suspensions were centrifuged at 8,000  $\times g$  (10 min, 4°C), washed three times with phosphate buffer saline (PBS) (pH 7.4), and the concentration of the bacterial solution was adjusted to  $10^9$  CFU/mL.

### Animal Experiments

All experiments were conducted in accordance with the National Institutes of Health guidelines for the care and use of experimental animals and approved by the Ethical Committee of the Experimental Animal Care of Beijing University of Agriculture (Beijing, China). Six-week-old male golden hamsters weighing  $110 \pm 20$  g/animal (Vital River, Beijing, China) were allowed to acclimatize for 1 week at a humidity of 45–50% and a temperature of  $20 \pm 2^\circ\text{C}$  and had free access to food and water. After acclimation in the feeding room for one week, the golden hamsters were randomly divided into four groups: Normal control group (Normal group), Model group (Model group), J-12 live bacteria group (J-12L), and J-12 heat-killed bacteria group (J-12D). There were six golden hamsters in the Normal group and 10 golden hamsters in other groups. The golden hamsters in the Normal and Model groups were gavaged with 1 mL sterile saline daily, the golden hamsters in the J-12L group were given  $10^9$  J-12 live bacteria by gavage, and the golden hamsters in the J-12D group were given  $10^9$  J-12 heat-killed bacteria by gavage. The golden hamsters were anesthetised by intraperitoneal injection of 10% (w/v) chloral hydrate (injection volume 0.3–0.5% body weight, J&K Scientific, Beijing, China) after 14 days of gavage. PBS buffer (0.25 mL) (pH = 7.4) was injected into the cheek pouches of the golden hamsters in the Normal group. The other three groups were injected with 0.25 mL methyl viologen dichloride (10 mmol/L, dissolved in PBS, Sigma-Aldrich, Missouri, USA) in cheek pouches. From the day of modelling until the golden hamsters were sacrificed, each group was given daily gavage intervention. On the fourth day after modelling, the golden hamsters were anesthetised, and the blood was collected. Then, the inside of the golden hamsters' mouth (except the ulcer site) was scraped with an oral swab, and the swab tip was cut and placed into a sample tube containing nucleic acid protection solution (Biobase, Shandong, China). Oral ulcer lesions or normal mucosa were cut and divided into two parts. One part was fixed in 4% paraformaldehyde, and the other part was frozen in liquid nitrogen. After separating the serum from whole blood, the serum was frozen at  $-80^\circ\text{C}$ .

### He Staining Sections Of Oral Ulcer Mucosal Tissues

Fixed oral ulcer mucosal tissues were embedded and sectioned in paraffin, then the sections were dewaxed and dehydrated, followed by haematoxylin and eosin staining, and finally dehydrated and

sealed for observation and photography under a microscope.

## **Immunohistochemical Slice Of Oral Ulcer In Areas Of Mucosal Tissue**

The paraffin section was dewaxed and dehydrated using citric acid antigen repair buffer (pH = 6.0), and then put into a 3% hydrogen peroxide solution with dark incubation for 25 min to block endogenous peroxidase. The next steps included primary antibody incubation (NF- $\kappa$ B, MMP-9, and caspase-3 antibodies (Proteintech, Wuhan, China); PARP antibodies (Boosen, Beijing, China)) and then secondary antibody incubation. Finally, after DAB colour development, nuclear counterstaining were performed; the slices were dehydrated and sealed, and then observed and photographed under a microscope.

Immunohistochemical scoring was done using the Immunoreactive Score scale. The degree of staining (0–3 points) and positive rate (0–4 points) were scored with the comprehensive score (0–12 points) obtained by multiplication. The degree of staining is scored according to the staining characteristics of the target protein: no staining is 0 points, light yellow is 1 point, brown yellow is 2 points, and tan is 3 points. The positive rate was scored according to the positive rate of cells in the section: 0–5% was 0 points, 6–25% was 1 point, 26–50% was 2 points, 51–75% was 3 points, and 75% was 4 points. Comprehensive score 0 was negative (-); 1–3 was weak positive (+); 3.1–5 was positive (+ +); and 5.1–7 was strongly positive (+ + +).

## **Determination Of Lxa4 And Pge2 In Mucous Tissues Of Oral Ulcers**

Oral mucous tissues of golden hamsters were collected to prepare tissue homogenates. LXA4 and PGE2 in tissue homogenates were measured by enzyme-linked immunosorbent assay (ELISA). The total protein concentration of tissue homogenate was measured to correct the contents of LXA4 and PGE2 (Huamei, Wuhan, China). The specific operation procedure was performed according to the corresponding kit instructions.

## **Serum Proinflammatory Cytokines And Oxidative Stress Indices Were Determined By Elisa**

The hamster's serum samples were quantified to evaluate the activity of inflammatory cytokine and interleukin markers using the IL-6 ELISA kit, IL-1 $\beta$  ELISA kit (BioSource International, California, USA), SOD ELISA kit, GSH ELISA kit, and malondialdehyde (MDA) ELISA kit (Betotime, Shanghai, China).

## **Determination Of Oral Microbiota Composition**

Total DNA was extracted from the oral swab samples of golden hamsters. Illumina PE300 sequencing platform was used for 16S rDNA high-throughput sequencing (Majorbio, Shanghai, China). The

sequencing data were subjected to OUT clustering, species annotation, diversity analysis, and other bioinformatics and data statistical analyses.

## Determination Of Intestinal Microbiota Composition

Total DNA was extracted from the colonic content samples of golden hamsters, and 16S rDNA high-throughput sequencing was performed by Illumina PE300 sequencing platform (Majorbio, Shanghai, China). The sequencing data were subjected to OUT clustering, species annotation, diversity analysis, and other bioinformatics and data statistical analyses.

## Statistical analysis

All experimental data were statistically analyzed using SPSS 26.0. Data were expressed as mean  $\pm$  standard deviation (SD) and analyzed by one-way analysis of variance (ANOVA). p-values  $< 0.05$  were considered statistically significant; \* denotes  $P < 0.05$ , \*\* denotes  $P < 0.01$ , and \*\*\* denotes  $P < 0.001$ .

## Declarations

### DATA AVAILABILITY

The data that support the findings of this study are available from the corresponding author upon reasonable request.

### Acknowledgments

This work was supported by Beijing Municipal Education Commission (KM202010020002) and Ningxia Hui Autonomous Region's key research and development plan "Research on strain breeding of the characteristic lactic acid bacteria and development key technology and industrial application of the functional yogurt product"(2020BBF02023).thank Dr. Zhan for her guidance during the animal experiments.

### AUTHOR CONTRIBUTIONS

All authors contributed to the research design. Conceptualization, Y.H. and N.J.; methodology, J.J. and R.W.; animal experiments, N.J. ,Y.Z. ,Y.H. and J.Y.; investigation, G.Y. and F.L.; data curation, J.J. and N.J.; writing-original draft preparation, J.J. and N.J.; writing-review and editing, J.J. and N.J. ; supervision, H.Z. Y.X. and H.L.All authors have read and agreed to the published version of the manuscript.

### COMPETING INTERESTS

The authors declare no competing interests.

## References

1. Avci, E., Akarlan, Z. Z., Erten, H. & Coskun-Cevher. S. Oxidative stress and cellular immunity in patients with recurrent aphthous ulcers. *Braz. J. Med. Biol. Res.* **47** 355–360 (2014).
2. Mumcu, G. & Fortune, F. Oral Health and Its Aetiological Role in Behçet's Disease. *Front Med-Lausanne* **8** 613419 (2021).
3. Seoudi, N. *et al.* The oral mucosal and salivary microbial community of Behçet's syndrome and recurrent aphthous stomatitis. *J. Oral Microbiol* **7** 27150 (2015).
4. Alshareef, A. *et al.* Effectiveness of Probiotic Lozenges in Periodontal Management of Chronic Periodontitis Patients: Clinical and Immunological Study. *European Journal of Dentistry* **14** 281–287 (2020).
5. Gerhard, D. *et al.* Probiotic therapy reduces inflammation and improves intestinal morphology in rats with induced oral mucositis. *Braz Oral Res* **31** e71 (2017).
6. Jiang, C. *et al.* A randomized, double-blind, placebo-controlled trial of probiotics to reduce the severity of oral mucositis induced by chemoradiotherapy for patients with nasopharyngeal carcinoma. *Cancer-Am Cancer Soc* **125** 1081–1090 (2019).
7. Li, D. *et al.* Efficacy and safety of probiotics in the treatment of Candida-associated stomatitis. *Mycoses* **57** 141–146 (2014).
8. Mimura, M. A. M., Borra, R. C., Hirata, C. H. W. & de Oliveira Penido, N. Immune response of patients with recurrent aphthous stomatitis challenged with a symbiotic. *J. Oral Pathol. Med.* **46** 821–828 (2017).
9. Zhang, H. *et al.* Bifidobacterium animalis ssp. Lactis 420 Mitigates Autoimmune Hepatitis Through Regulating Intestinal Barrier and Liver Immune Cells. *Front Immunol* **11** 569104 (2020).
10. Li, S. C., Hsu, W. F., Chang, J. S. & Shih, C. K. Combination of Lactobacillus acidophilus and Bifidobacterium animalis subsp. lactis Shows a Stronger Anti-Inflammatory Effect than Individual Strains in HT-29 Cells. *Nutrients* **11** 969 (2019).
11. Wang, N. *et al.* Alleviation Effects of Bifidobacterium animalis subsp. lactis XLTG11 on Dextran Sulfate Sodium-Induced Colitis in Mice. *Microorganisms* **9** 2093 (2021).
12. Shen, Q., Shang, N. & Li, P. In Vitro and In Vivo Antioxidant Activity of Bifidobacterium animalis 01 Isolated from Centenarians. *Curr. Microbiol.* **62** 1097–1103 (2011).
13. Adams, C. A. The probiotic paradox: live and dead cells are biological response modifiers. *Nutr. Res. Rev.* **23** 37–46 (2010).
14. Taverniti, V. & Guglielmetti, S. The immunomodulatory properties of probiotic microorganisms beyond their viability (ghost probiotics: proposal of paraprotibiotic concept). *Genes & nutrition* **6** 261–274 (2011).
15. Chen, Q. M., Li, B. Q. & Xiao, Z. R. A Reearch on the Damage of Oxygen Free Radicals to the Oral Mucosa of Animal (I) — Establishment of Animal Model. *West China Journal of Stomatology* **11** 62–64 (1993).

16. Wang, Y., Branicky, R., Noë, A. & Hekimi, S. Superoxide dismutases: Dual roles in controlling ROS damage and regulating ROS signaling. *The Journal of cell biology* **217** 1915–1928 (2018).
17. Fraternali, A., Brundu, S. & Magnani, M. Glutathione and glutathione derivatives in immunotherapy. *Biol. Chem.* **398** 261 (2017).
18. Clara J. Busch, C. J. B. Malondialdehyde epitopes as mediators of sterile inflammation. *BBA - Molecular and Cell Biology of Lipids* **1862** 398–406 (2016).
19. Serhan, C. N., Chiang, N. & Van Dyke, T. E. Resolving inflammation: dual anti-inflammatory and pro-resolution lipid mediators. *Nat. Rev. Immunol.* **8** 349–361 (2008).
20. Zhang, S. *et al.* Prostaglandin E2 hydrogel improves cutaneous wound healing via M2 macrophages polarization. *Theranostics* **8** 5348–5361 (2018).
21. Richard, K., Ines, D., Grant, N.W. & Dylan, R. E. The ADAMTS (A Disintegrin and Metalloproteinase with Thrombospondin motifs) family. *Genome Biology* **16** 113 (2015).
22. Tanaka, T., Narazaki, M. & Kishimoto, T. Interleukin (IL-6) Immunotherapy. *Csh Perspect Biol* **10** a28456 (2018).
23. Park, J. H. *et al.* Melittin suppresses PMA-induced tumor cell invasion by inhibiting NF- $\kappa$ B and AP-1-dependent MMP-9 expression. *Mol. Cells* **29** 209–215 (2010).
24. Wooten, M. W. Function for NF- $\kappa$ B in Neuronal Survival: Regulation by Atypical Protein Kinase C. *J. Neurosci. Res.* **58** 607–611 (1999).
25. Al-Sadi, R. *et al.* Matrix Metalloproteinase-9 (MMP-9) induced disruption of intestinal epithelial tight junction barrier is mediated by NF- $\kappa$ B activation. *Plos One* **16** e249544 (2021).
26. Jeong, C. H. *et al.* Effects of Aluminum on the Integrity of the Intestinal Epithelium: An in Vitro and in Vivo Study. *Environ. Health Persp.* **128** 17013 (2020).
27. Jang, H. *et al.* 15d-PGJ 2 inhibits NF- $\kappa$ B and AP-1-mediated MMP-9 expression and invasion of breast cancer cell by means of a heme oxygenase-1-dependent mechanism. *Bmb Rep* **53** 212–217 (2020).
28. Schenck, K., Schreurs, O., Hayashi, K. & Helgeland, K. The Role of Nerve Growth Factor (NGF) and Its Precursor Forms in Oral Wound Healing. *International Journal of Molecular Sciences* **18** 386 (2017).
29. Vijayakumar, E. C., Bhatt, L. K. & Prabhavalkar, K. S. High Mobility Group Box-1 (HMGB1): A Potential Target in Therapeutics. *Curr. Drug Targets* **20** 1474–1485 (2019).
30. Yan, X. X. *et al.* Increased serum HMGB1 level is associated with coronary artery disease in nondiabetic and type 2 diabetic patients. *Atherosclerosis* **205** 544–548 (2009).
31. Kigerl, K. A. *et al.* High mobility group box-1 (HMGB1) is increased in injured mouse spinal cord and can elicit neurotoxic inflammation. *Brain, Behavior, and Immunity* **72** 22–33 (2018).
32. Yang, R. *et al.* Bile and circulating HMGB1 contributes to systemic inflammation in obstructive jaundice. *J. Surg. Res.* **228** 14–19 (2018).
33. Shang, G. *et al.* Serum high mobility group box protein 1 as a clinical marker for non-small cell lung cancer. *Resp. Med.* **103** 1949–1953 (2009).



34. Liu, B. M. *et al.* Baicalein protects Human melanocytes from H<sub>2</sub>O<sub>2</sub>-induced apoptosis via inhibiting mitochondria-dependent caspase activation and the p38 MAPK pathway. *Free Radical Bio. Med.* **53** 183–193 (2012).
35. Danial, N. N. BCL-2 Family Proteins: Critical Checkpoints of Apoptotic Cell Death. *Clin. Cancer Res.* **13** 7254–7263 (2007).
36. Jin, J. S. *et al.* Smokeless tobacco impacts oral microbiota in a Syrian Golden hamster cheek pouch carcinogenesis model. *Anaerobe* **52** 29–42 (2018).
37. Tremaroli, V. & Bäckhed, F. Functional interactions between the gut microbiota and host metabolism. *Nature* **489** 242–249 (2012).
38. Lukic, J. *et al.* Probiotics or pro-healers: the role of beneficial bacteria in tissue repair. *Wound Repair Regen.* **25** 912–922 (2017).
39. Roy, S., Amin, S. & Roy, S. Retinal fibrosis in diabetic retinopathy. *Exp. Eye Res.* **142** 71–75 (2016).
40. Pang, X. *et al.* Microbiota, Epithelium, Inflammation, and TGF- $\beta$  Signaling: An Intricate Interaction in Oncogenesis. *Front Microbiol* **9** 1353 (2018).
41. TAGLIARI, E. *et al.* EFFECT OF PROBIOTIC ORAL ADMINISTRATION ON SKIN WOUND HEALING IN RATS. *Arquivos Brasileiros de Cirurgia Digestiva (São Paulo)* **32** e1457 (2019).
42. Varian, B. J. *et al.* Microbial lysate upregulates host oxytocin. *Brain, Behavior, and Immunity* **61** 36–49 (2017).
43. Su, X. *et al.* San-Huang-Yi-Shen Capsule Ameliorates Diabetic Nephropathy in Rats Through Modulating the Gut Microbiota and Overall Metabolism. *Front Pharmacol* **12** 808867 (2022).
44. Baker, J. L. *et al.* Ecology of the Oral Microbiome: Beyond Bacteria. *Trends Microbiol.* **25** 362–374 (2017).
45. Sun, J. *et al.* Role of the oral microbiota in cancer evolution and progression. *Cancer Med-Us* **9** 6306–6321 (2020).
46. Fujiwara, N. *et al.* Involvement of Fusobacterium Species in Oral Cancer Progression: A Literature Review Including Other Types of Cancer. *International Journal of Molecular Sciences* **21** 6207 (2020).
47. Aadra P. Bhatt, M. R. R. S. The Role of the Microbiome in Cancer Development and Therapy. *CA: a cancer journal for clinicians* **67** 326–344 (2017).
48. Niu, L. *et al.* Isolation and characterization of *Streptococcus respiraculi* sp. nov. from *Marmota himalayana* (Himalayan marmot) respiratory tract. *Int. J. Syst. Evol. Micr.* **68** 2082–2087 (2018).
49. Bakir, M. A. *et al.* *Bacteroides dorei* sp. nov., isolated from human faeces. *Int. J. Syst. Evol. Micr.* **56** 1639–1643 (2006).
50. Yoshida, N. *et al.* *Bacteroides vulgatus* and *Bacteroides dorei* Reduce Gut Microbial Lipopolysaccharide Production and Inhibit Atherosclerosis. *Circulation* **138** 2486–2498 (2018).
51. Song, L. *et al.* A Novel Immunobiotics *Bacteroides dorei* Ameliorates Influenza Virus Infection in Mice. *Front Immunol* **12** 828887 (2022).

52. Gao, G. *et al.* BdPUL12 depolymerizes  $\beta$ -mannan-like glycans into mannooligosaccharides and mannose, which serve as carbon sources for *Bacteroides dorei* and gut probiotics. *Int. J. Biol. Macromol.* **187** 664–674 (2021).
53. Che, Q. *et al.* Mechanisms by Which Traditional Chinese Medicines Influence the Intestinal Flora and Intestinal Barrier. *Front Cell Infect Mi* **12** 863779 (2022).
54. Quan, T. *et al.* *Ficus hirta* Vahl. Ameliorates Nonalcoholic Fatty Liver Disease through Regulating Lipid Metabolism and Gut Microbiota. *Oxid Med Cell Longev* **2022** 1–31 (2022).
55. Everard, A. *et al.* Microbiome of prebiotic-treated mice reveals novel targets involved in host response during obesity. *The ISME Journal* **8** 2116–2130 (2014).
56. Zhao, J. *et al.* Effect of berberine on hyperglycaemia and gut microbiota composition in type 2 diabetic Goto-Kakizaki rats. *World J. Gastroentero.* **27** 708–724 (2021).
57. Balakrishnan, B. *et al.* *Prevotella histicola* Protects From Arthritis by Expansion of *Allobaculum* and Augmenting Butyrate Production in Humanized Mice. *Front Immunol* **12** 609644 (2021).
58. Shao, T. *et al.* Combined Signature of the Fecal Microbiome and Metabolome in Patients with Gout. *Front Microbiol* **8** 268 (2017).
59. Bruna, C. D. S. C. *et al.* Use of the synbiotic VSL#3 and yacon-based concentrate attenuates intestinal damage and reduces the abundance of *Candidatus Saccharimonas* in a colitis-associated carcinogenesis model. *Food research international (Ottawa, Ont.)* **137** 109721 (2020).
60. Wang, Y. *et al.* Dietary Supplementation of Inulin Ameliorates Subclinical Mastitis via Regulation of Rumen Microbial Community and Metabolites in Dairy Cows. *Microbiol Spectr* **9** e10521 (2021).

## Table

Table 2 is not available with this version.

## Figures

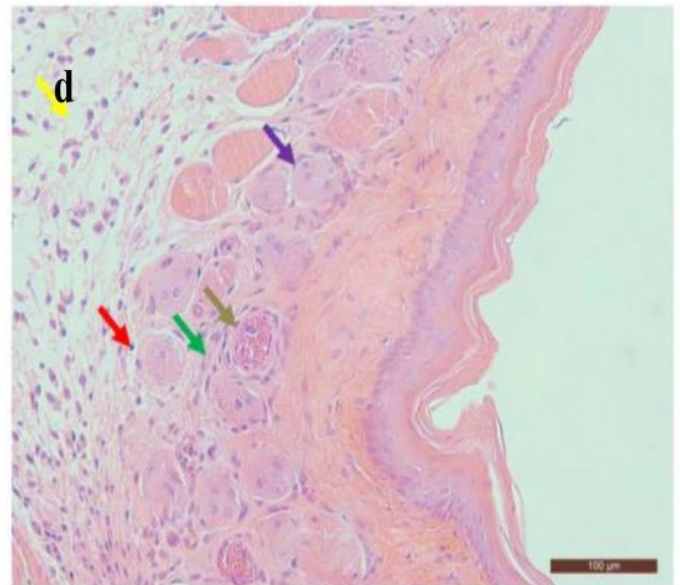
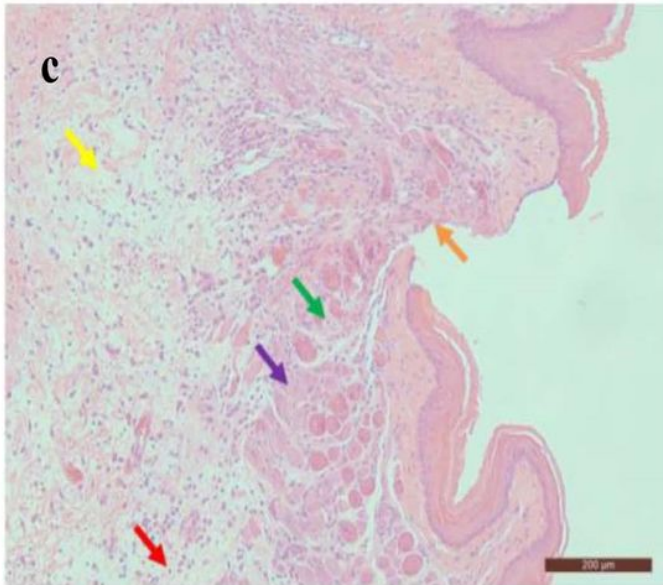
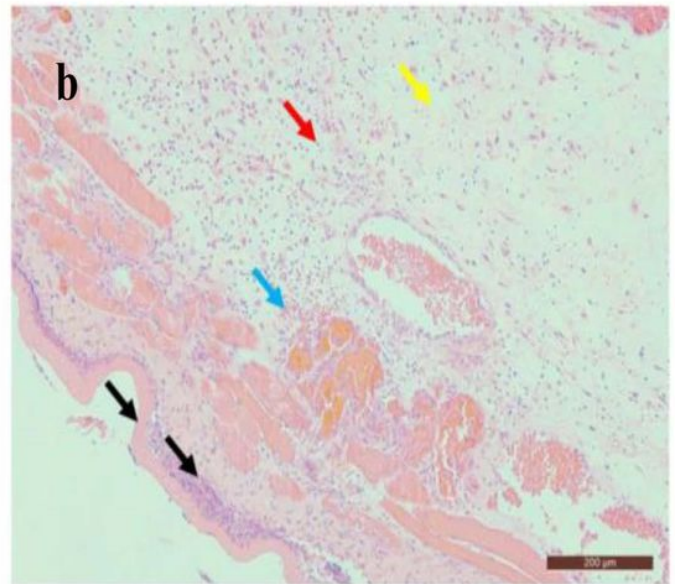
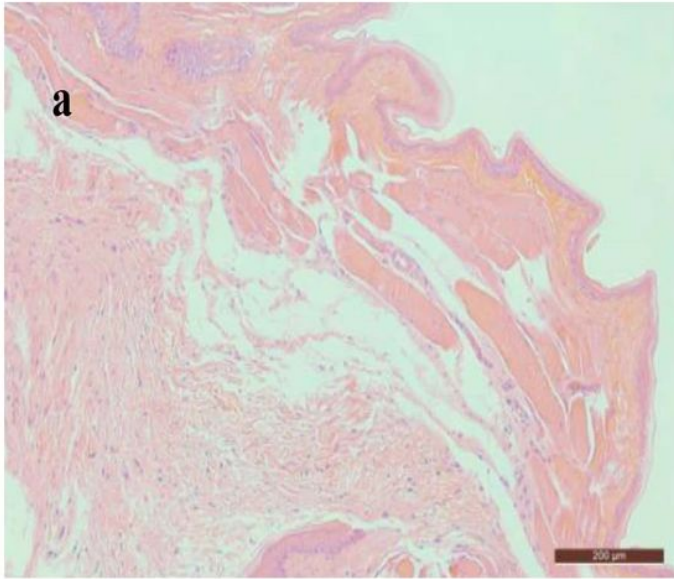


**Figure 1**

**HE staining images of typical golden hamsters oral mucosal tissue sections. a** Normal group, **b** Model group, **c** J-12 L group, **d** J-12 group.

The red arrow points to inflammatory cell infiltration. The black arrow points to mucosal epithelial cell necrosis and nuclear fragmentation. The yellow arrow points to loose arrangement of connective tissue. The blue arrow points to bleeding. The purple arrow points in the direction of new muscle fibres. The green arrow points to the connective tissue hyperplasia. The brown arrows point to capillary congestion dilation. The orange arrows point to local epidermal layer loss (Normal group, Model scale group: 200 µm, J-12L group, and J-12D group scale: 100 µm).

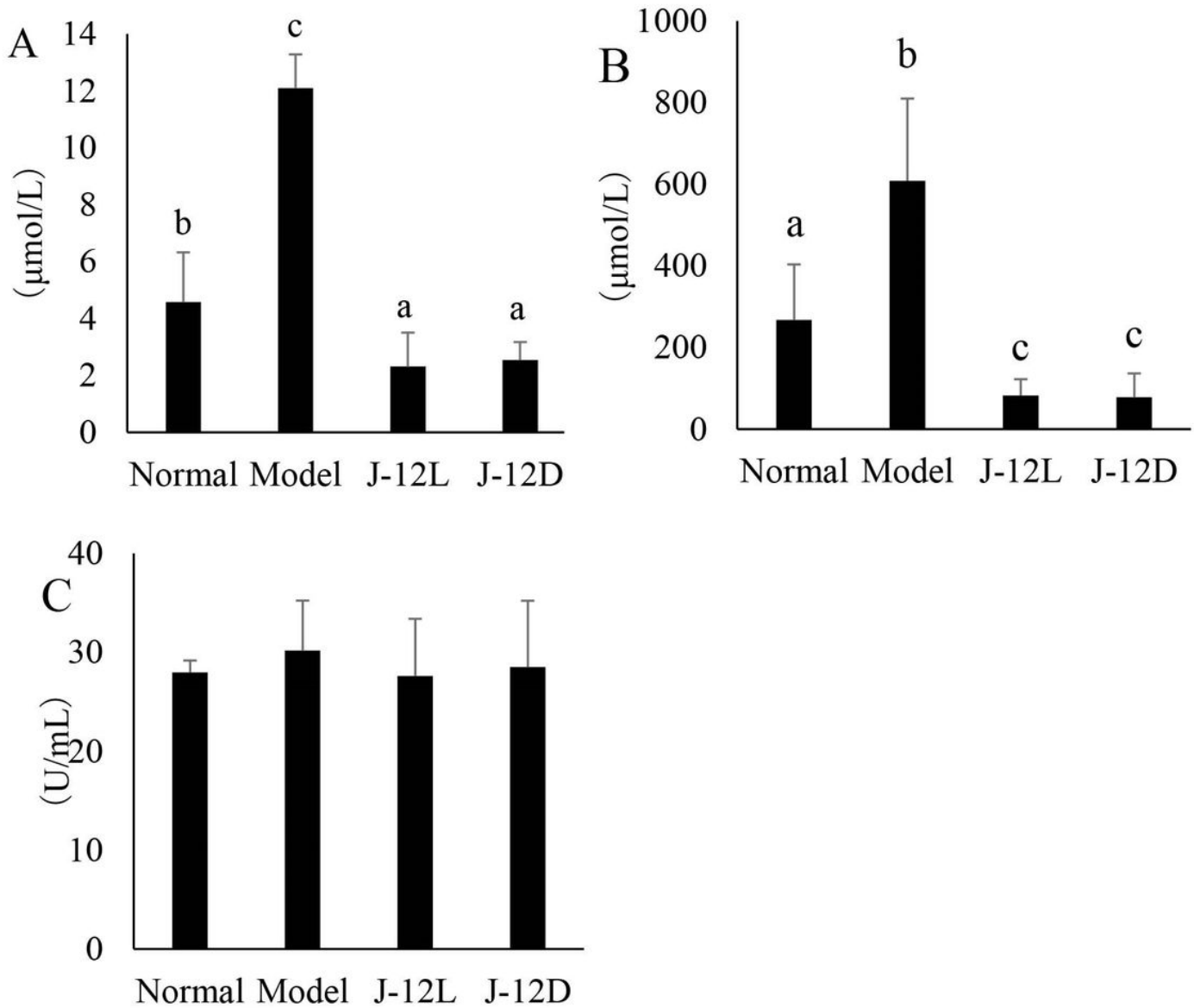


**Figure 2**

**Level of oxidation index in serum of golden hamsters. A** level of GSH; **B** level of MDA; **C** level of SOD. Data are shown as mean  $\pm$  standard deviation. One-way ANOVA was used to analyze statistical differences. Different letters at the top of the column indicating significant differences ( $P < 0.05$ ).

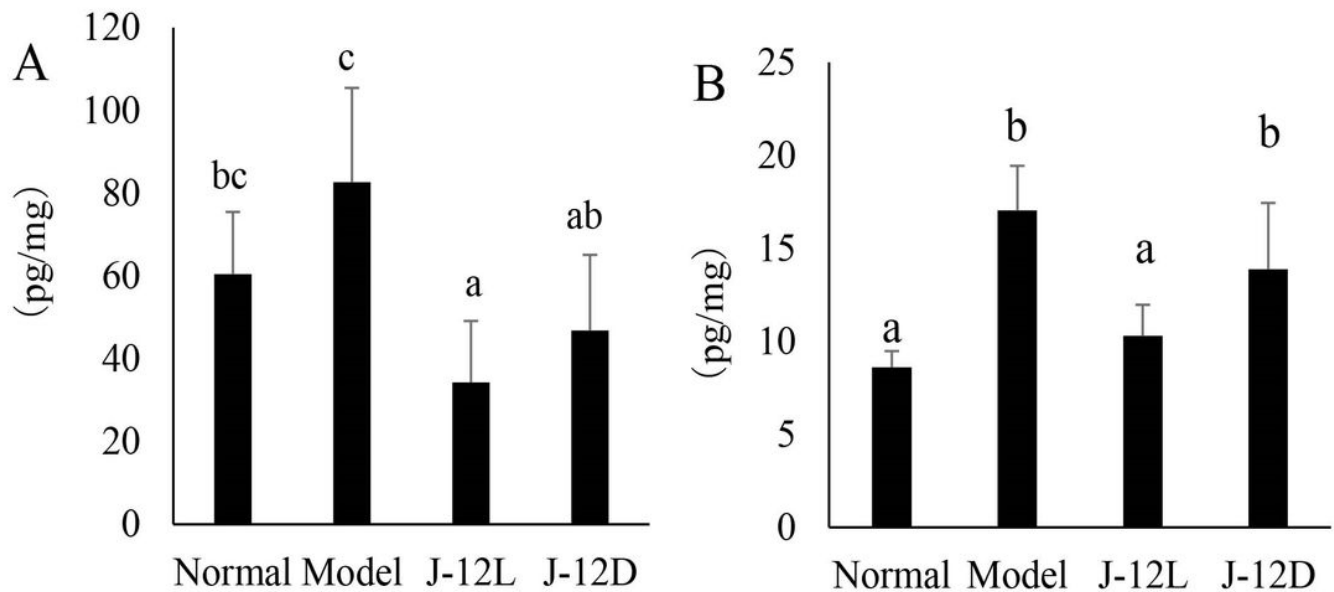


**Figure 3**

**Levels of antioxidant factors in mucosal tissues of golden hamsters. A** level of LXA4; **B** level of PGE2.

Data are shown as mean  $\pm$  standard deviation. One-way ANOVA was used to analyze statistical differences. Different letters at the top of the column indicating significant differences ( $P < 0.05$ ).

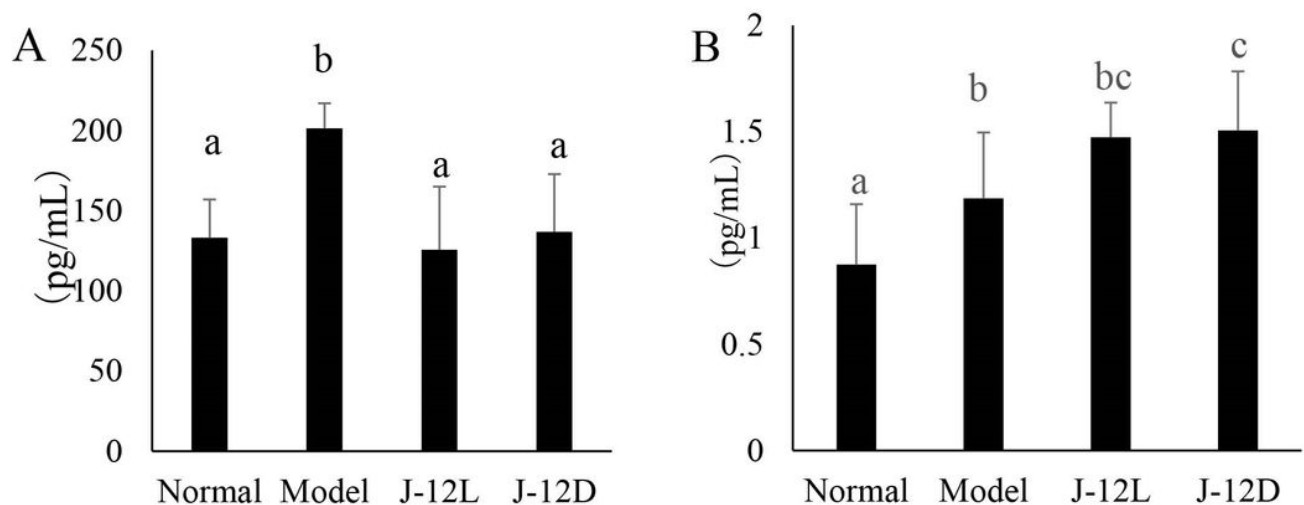


**Figure 4**

**Levels of proinflammatory factor in serum of golden hamsters. A** IL-1 $\beta$ , **B**IL-6. Data are shown as mean  $\pm$

standard deviation. One-way ANOVA was used to analyze statistical differences. Different letters at the top of the column indicating significant differences ( $P < 0.05$ ).

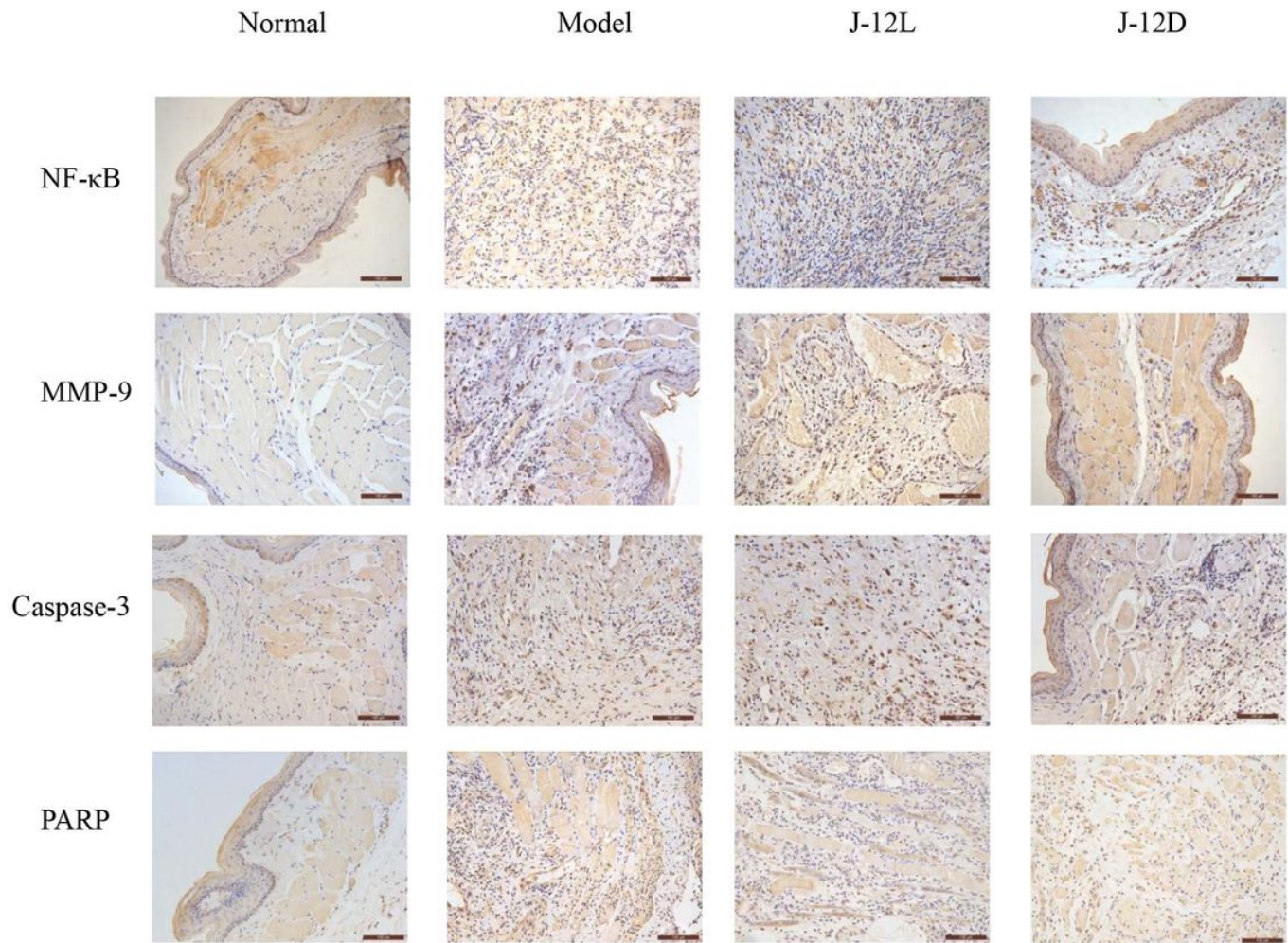


**Figure 5**

Typical immunohistochemical images in the mucosa tissue of golden hamster (scale: 100  $\mu$ m)

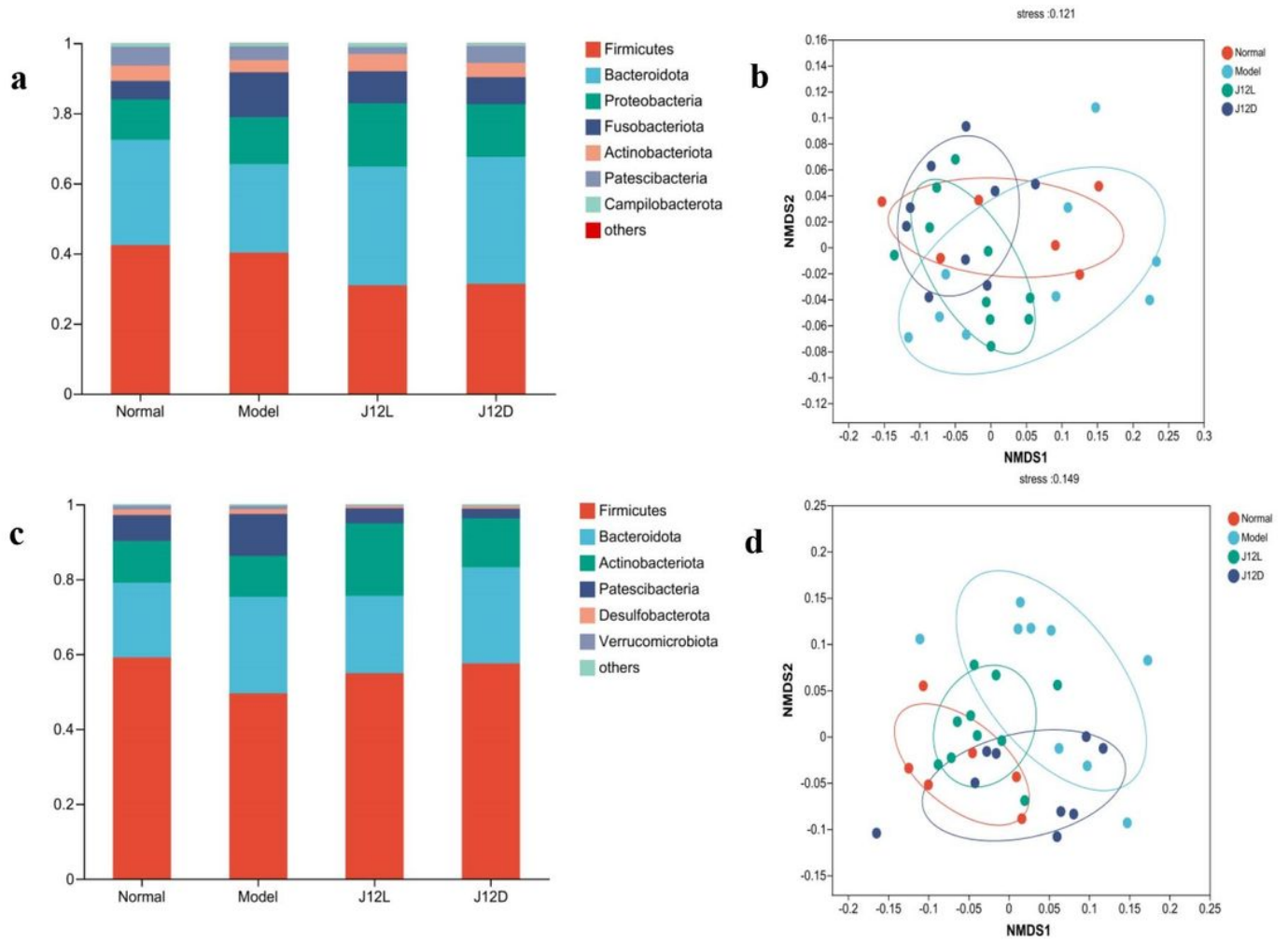


**Figure 6**

**J-12 altered the flora structure of golden hamsters. a** community composition of oral microbiota at the phylum level; **b** community composition of intestinal microbiota at the phylum level; **c** species level NMDS map of oral microbiota; **d** species level NMDS map of intestinal microbiota.

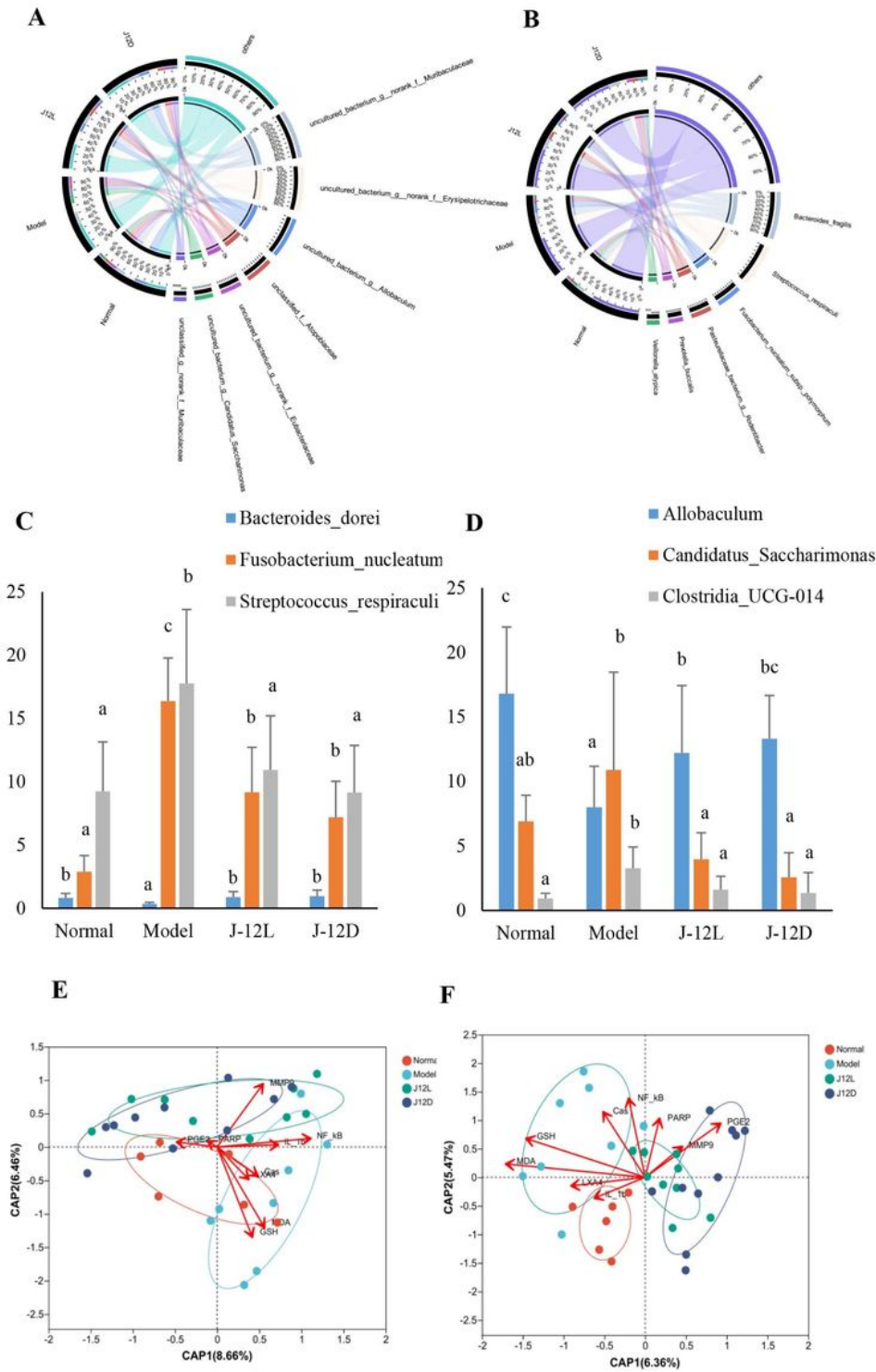


**Figure 7**

**J-12 altered the relative abundance of dominant bacteria of golden hamsters.** **A** visualization circle of oral bacteria; **B** visualization circle of intestinal bacteria; **C** the relative abundance of oral dominant bacteria with significant differences; **D** the relative abundance of intestinal dominant bacteria with significant differences; **E** db-RDA of oral microbiota species level in golden hamsters; **F** db-RDA of intestinal microbiota species level in golden hamsters. Data are shown as mean  $\pm$  standard deviation.



One-way ANOVA was used to analyze statistical differences. Different letters at the top of the column of the same strain indicating significant differences ( $P < 0.05$ ).

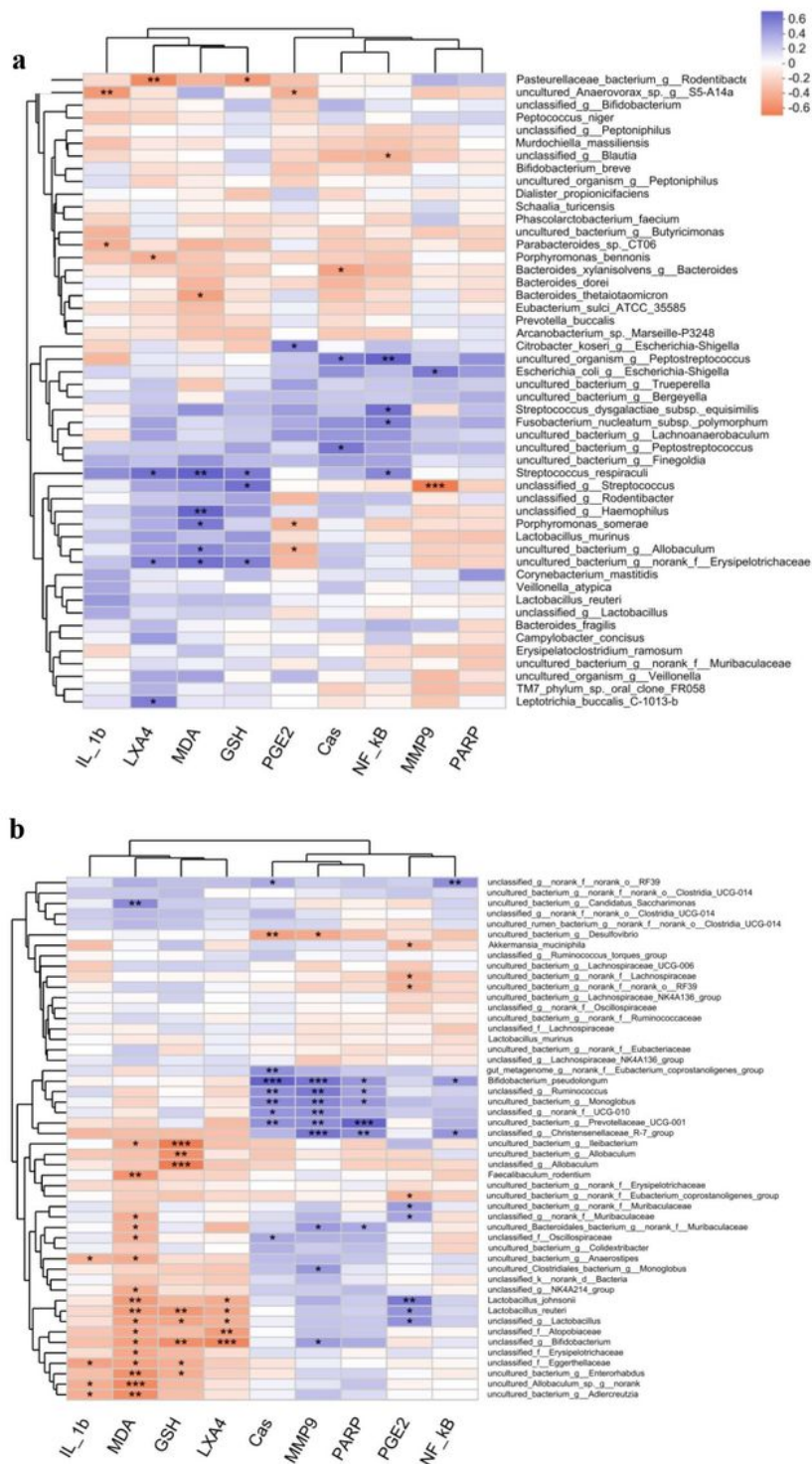


Figure 8

Heat map of correlation between species and factors in golden hamsters. **a** heat map of correlation between oral flora and factors in golden hamsters; **b** heat map of correlation between intestinal and

factors in golden hamsters. Spearman was used to analyze statistical differences. \* denotes  $P < 0.05$ , \*\* denotes  $P < 0.01$ , and \*\*\* denotes  $P < 0.001$ .